

Network Realization Functions for Optimal Distributed Control

Șerban Sabău[‡], Andrei Sperilă[‡], Cristian Oară[‡] and Ali Jadbabaie[‡]

Abstract—In this paper, we discuss a distributed control architecture, aimed at networks with linear and time-invariant dynamics, which is amenable to convex formulations for controller design. The proposed approach is well suited for large scale systems, since the resulting feedback schemes completely avoid the exchange of internal states, i.e., plant or controller states, among sub-controllers. Additionally, we provide state-space formulas for these sub-controllers, able to be implemented in a distributed manner.

Index Terms—Distributed control, linear time-invariant networks, scalable implementations.

I. INTRODUCTION

A. Scope of Work

The multi-faceted intricacies of the optimal decentralized control problem are widely recognized in literature. With the hope for the existence of any convenient (let alone convex) parameterizations dispelled (see, for example, [1]), recent research advances have resorted to modern convexification or regularization methods, such as [2], [3], [4], [5], [6]. In this context, the so-called *System Level Synthesis* (SLS) methods from [7], [8] provided an insightful perspective on distributed controller design, by exploiting the classical work from [9]. The connections between SLS and classical parameterizations of stabilizing controllers have been further elaborated upon in [10], [11] and, more recently, in [12] (see also the literature review from the introduction of our companion paper [13]).

However, the SLS framework: (a) necessitates implementations which communicate internal states, i.e., controller or plant states, thus producing Transfer Function Matrices (TFM) of the controller's representation with dimensions equal to that of the plant's state vector, while (b) allowing for the direct application (see the concluding remark of Section II-B in [14]) of the scalable, *specialized implementations* from Section III-C of [8] only for networks which have open-loop stable plants.

B. Problem Statement and Contributions

The paper tackles the problem of obtaining a set of stabilizing and distributed control laws of the type

$$u = \Phi u + \Gamma z,$$

[‡] Șerban Sabău is with the Electrical and Computer Engineering Department, Stevens Institute of Technology, Hoboken, NJ 07030 USA (e-mail: ssabau@stevens.edu).

[‡] Andrei Sperilă and Cristian Oară are with the Faculty of Automatic Control and Computers, "Politehnica" University of Bucharest, Sector 6, 060042 Romania (e-mails: {andrei.sperila, cristian.oara}@upb.ro).

[‡] Ali Jadbabaie is with the Institute for Data, Systems and Society, Massachusetts Institute of Technology (MIT), Cambridge, MA 02139 USA (email: jadbabai@mit.edu).

The work of Șerban Sabău was supported by the NSF - CAREER under Grant 1653756. The work of Andrei Sperilă and Cristian Oară was supported by a grant of the Ministry of Research, Innovation and Digitization, CCCDI - UEFISCDI, project no. PN-III-P2-2.1-PED-2021-1626, within PNCDI III. The work of Ali Jadbabaie was supported by the Vannevar Bush Fellowship from the Office of the Secretary of Defense.

where the pair of LTI (Linear Time Invariant) filters (Φ, Γ) showcase pre-specified sparsity patterns and are used to compute the command signals, u , via the regulated measurements, z , without communicating any internal states between sub-controllers. The main contributions of our work are as follows:

- 1) providing a general method of obtaining distributed control laws that are akin to the *specialized implementations* presented in Section III-C of [8];
- 2) bypassing the drawbacks mentioned in points (a) and (b), while guaranteeing the full scalability of the distributed control laws, for possibly unstable plants;
- 3) obtaining control laws for both discrete- and continuous-time (see [13], [15]) systems, while completely avoiding any self-loops (either integrators or delay elements) on the control signals, thus facilitating implementation.

We point out that the proposed method relies on the concept of Network Realization Functions (NRF), heavily inspired by the work in [16] and [17], which is able to impose sparsity patterns directly on the distributed controller's coprime factors. The close affinity between these factorizations and NRFs (see [18]) enables the exploitation of the robust stabilization machinery for distributed controller design, as established in [13].

C. Paper Structure

In Section II, we present the concept of NRF pairs, all while showcasing their defining traits. In Section III, we discuss the means of enforcing sparsity patterns upon an NRF pair, in the same vein as the approach from [19], and we offer guarantees of closed-loop stability when implementing controllers via this formalism. We also present the means to obtain distributed state-space implementations for our controllers' NRF pairs, in contrast to the purely TFM-based perspective from [19], and we show that norm-based optimal design in the NRF paradigm reduces to an affine model matching problem (see also [13]). In Section IV, we discuss alternative representations for our distributed control laws, akin to and inspired by the ones in [7] and [8], which use closed-loop maps to compute the command signals. We show that, unlike the architecture from Section III, these cannot ensure closed-loop stability if the plant does not satisfy certain stability assumptions (as in Section III-C of [8]). Section V showcases a numerical example (see also Section V of [13]), while Section VI contains a number of conclusions.

II. GENERAL SETUP AND TECHNICAL PRELIMINARIES

A. Notation

Since the enclosed results are valid for both continuous- and discrete-time LTI systems, we denote by λ the complex variable associated with the Laplace transform for continuous-time systems, or with the \mathcal{Z} -transform for discrete-time ones.

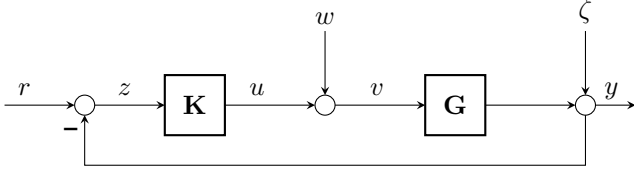


Fig. 1. Feedback loop of the plant G with the controller K

We denote by \mathbb{R} the set of real numbers and by \mathbb{N} the set of natural ones, while \mathbb{C} stands for the complex plane. Let $\mathbb{R}^{p \times m}$ be the set of $p \times m$ real matrices and $\mathbb{R}(\lambda)^{p \times m}$ the set of $p \times m$ TFMs, matrices with real-rational functions as entries. Let e_i stand for the i^{th} vector in the canonical basis of $\mathbb{R}^{m \times 1}$. A TFM for which $\lim_{\lambda \rightarrow \infty} G(\lambda)$ has only finite entries is called proper and it is called strictly proper when $\lim_{\lambda \rightarrow \infty} G(\lambda) = O$. We denote by $\mathbb{R}_p(\lambda)^{p \times m}$ the set of proper TFMs. Finally, let \mathbb{S} denote the domain of stability, which is either the open left-half plane ($\text{Re}(\lambda) < 0$, $\lambda \in \mathbb{C}$) for continuous-time systems or the open unit disk ($|\lambda| < 1$, $\lambda \in \mathbb{C}$) for discrete-time ones.

B. TFM and Realization Theory

The LTI systems considered in this paper are described in the time domain by the classical state-space equations

$$\sigma x = Ax + Bu, \quad (1a)$$

$$y = Cx + Du, \quad (1b)$$

where $A \in \mathbb{R}^{n \times n}$, $B \in \mathbb{R}^{n \times m}$, $C \in \mathbb{R}^{p \times n}$ and $D \in \mathbb{R}^{p \times m}$, and n is called the *order* of the realization. The time-domain operator denoted by σ in (1a)-(1b) stands for either the time derivative (in the continuous-time context) or the forward unit-shift (in the discrete-time case). For any n -dimensional state-space realization (1a)-(1b), the system's TFM is given by

$$G(\lambda) = \left[\begin{array}{c|c} A - \lambda I_n & B \\ \hline C & D \end{array} \right] := D + C(\lambda I_n - A)^{-1}B.$$

We denote by $\mathcal{P}_u(G)$ the collection of (finite) unstable poles (see Section 6.5.3 of [20]), *i.e.*, located in $\mathbb{C} \setminus \mathbb{S}$, which belong to $G \in \mathbb{R}_p(\lambda)^{p \times m}$. We refer to $G \in \mathbb{R}_p(\lambda)^{p \times m}$ as *stable* if $\mathcal{P}_u(G) = \{\emptyset\}$ and we denote the set of these TFMs by $\mathbb{R}_s(\lambda)^{p \times m} (\subset \mathbb{R}_p(\lambda)^{p \times m})$. Otherwise, we say that it is *unstable*. Note that $\mathcal{P}_u(G)$ includes repeated terms when the unstable poles of G have multiplicities greater than 1. Furthermore, we denote by $\Lambda_u(A)$ the collection of eigenvalues belonging to the matrix A which are unstable, *i.e.*, located in $\mathbb{C} \setminus \mathbb{S}$. Once again, $\Lambda_u(A)$ includes repeated terms when the unstable eigenvalues of A have multiplicities greater than 1.

C. Standard Unity Feedback

We focus on the standard unity feedback of Fig. 1, where $G \in \mathbb{R}_p(\lambda)^{p \times m}$ is the LTI plant and $K \in \mathbb{R}_p(\lambda)^{m \times p}$ is its LTI controller. Here r , w and ζ are the reference signal, input disturbance and sensor noise vectors, respectively, while y , u , z and v are the measurement, command, regulated and applied control signal vectors, respectively. If all the closed-loop maps from the exogenous signals $[r^\top \ w^\top \ \zeta^\top]^\top$ to $[y^\top \ u^\top \ z^\top \ v^\top]^\top$, *i.e.*, any point inside the feedback loop of Fig. 1, are stable then we say that K is an (internally) stabilizing controller of G or that K (internally) stabilizes G .

D. The Youla Parametrization

The seminal work presented in [21] highlighted the fact that the problem of closed-loop stabilization can be conveniently reformulated in terms of particular fractional representations, belonging to the TFMs which make up the feedback control scheme. In this context, we introduce several key definitions.

Definition II.1. Let $K \in \mathbb{R}_p(\lambda)^{m \times p}$, $R \in \mathbb{R}_p(\lambda)^{m \times m}$, $P \in \mathbb{R}_p(\lambda)^{m \times p}$. A representation of the form $K = R^{-1}P$ is called a left factorization of K .

Remark II.2. If $K = Y^{-1}X$ is a left factorization of K , then any other left factorization of K (as in Definition II.1) is of the form $R = UY$, $P = UX$, for some invertible TFM U .

Definition II.3 (Corollary 4.1.4 in [21]). A left factorization $G = \tilde{M}^{-1}\tilde{N} \in \mathbb{R}_p(\lambda)^{p \times m}$ with $\tilde{N} \in \mathbb{R}_s(\lambda)^{p \times m}$, $\tilde{M} \in \mathbb{R}_s(\lambda)^{p \times p}$ is additionally called coprime over $\mathbb{R}_s(\lambda)$ if there exist $\tilde{X} \in \mathbb{R}_s(\lambda)^{m \times p}$, $\tilde{Y} \in \mathbb{R}_s(\lambda)^{p \times p}$ so that $\tilde{M}\tilde{Y} + \tilde{N}\tilde{X} = I_p$.

Remark II.4. Note also that a right coprime factorization over $\mathbb{R}_s(\lambda)$ of G can be obtained in a straightforward fashion by simply transposing the left coprime factors over $\mathbb{R}_s(\lambda)$ of G^\top .

Definition II.5. (Remark 4.1.17 in [21]) A collection of eight stable TFMs $(M, N, \tilde{M}, \tilde{N}, X, Y, \tilde{X}, \tilde{Y})$ is called a doubly coprime factorization (DCF) over $\mathbb{R}_s(\lambda)$ of $G \in \mathbb{R}_p(\lambda)^{p \times m}$ if \tilde{M} and M are both invertible, they yield the factorizations $G = \tilde{M}^{-1}\tilde{N} = NM^{-1}$ and they satisfy the following equality

$$\begin{bmatrix} Y & X \\ -\tilde{N} & \tilde{M} \end{bmatrix} \begin{bmatrix} M & -\tilde{X} \\ N & \tilde{Y} \end{bmatrix} = I_{m+p}. \quad (2)$$

The next theorem provides, via such DCFs over $\mathbb{R}_s(\lambda)$, the parameterization of *all* stabilizing controllers for a given plant.

Theorem II.6 (Theorem 5.2.1 in [21]). Let $(M, N, \tilde{M}, \tilde{N}, X, Y, \tilde{X}, \tilde{Y})$ be a DCF over $\mathbb{R}_s(\lambda)$ of $G \in \mathbb{R}_p(\lambda)^{p \times m}$. Define

$$\begin{aligned} X_Q &:= X + Q\tilde{M}, & \tilde{X}_Q &:= \tilde{X} + MQ, \\ Y_Q &:= Y - Q\tilde{N}, & \tilde{Y}_Q &:= \tilde{Y} - NQ, \end{aligned} \quad (3)$$

for some $Q \in \mathbb{R}_s(\lambda)^{m \times p}$, and note also that the following generalization of the identity from (2) holds

$$\begin{bmatrix} Y_Q & X_Q \\ -\tilde{N} & \tilde{M} \end{bmatrix} \begin{bmatrix} M & -\tilde{X}_Q \\ N & \tilde{Y}_Q \end{bmatrix} = I_{m+p}. \quad (4)$$

Then, the class of all controllers K_Q which stabilize the plant G (in feedback interconnection, see Fig. 1) is given by

$$K_Q = Y_Q^{-1}X_Q = \tilde{X}_Q\tilde{Y}_Q^{-1} \in \mathbb{R}(\lambda)^{m \times p}, \quad (5)$$

for all $Q \in \mathbb{R}_s(\lambda)^{m \times p}$ which ensure that both Y_Q and \tilde{Y}_Q are invertible TFMs.

Denote by $H_{CL}(G, K_Q)$ the TFM from $[r^\top \ w^\top \ \zeta^\top]^\top$ to $[y^\top \ u^\top \ z^\top \ v^\top]^\top$, whose entries are the achievable closed-loop maps produced by stabilizing controllers (5) and which are given explicitly in (6), at the top of the next page. One of the chief features of the Youla Parameterization is the fact that it renders all closed-loop maps from the feedback loop in Fig. 1 as *affine expressions* of the free (and stable) parameter Q , as highlighted via the following result.

$$\mathbf{H}_{CL}(\mathbf{G}, \mathbf{K}_Q) := \begin{bmatrix} (I_p + \mathbf{G}\mathbf{K}_Q)^{-1}\mathbf{G}\mathbf{K}_Q & (I_p + \mathbf{G}\mathbf{K}_Q)^{-1}\mathbf{G} & (I_p + \mathbf{G}\mathbf{K}_Q)^{-1} \\ (I_m + \mathbf{K}_Q\mathbf{G})^{-1}\mathbf{K}_Q & -(I_m + \mathbf{K}_Q\mathbf{G})^{-1}\mathbf{K}_Q\mathbf{G} & -(I_m + \mathbf{K}_Q\mathbf{G})^{-1}\mathbf{K}_Q \\ (I_p + \mathbf{G}\mathbf{K}_Q)^{-1} & -(I_p + \mathbf{G}\mathbf{K}_Q)^{-1}\mathbf{G} & -(I_p + \mathbf{G}\mathbf{K}_Q)^{-1} \\ (I_m + \mathbf{K}_Q\mathbf{G})^{-1}\mathbf{K}_Q & (I_m + \mathbf{K}_Q\mathbf{G})^{-1} & -(I_m + \mathbf{K}_Q\mathbf{G})^{-1}\mathbf{K}_Q \end{bmatrix} \quad (6)$$

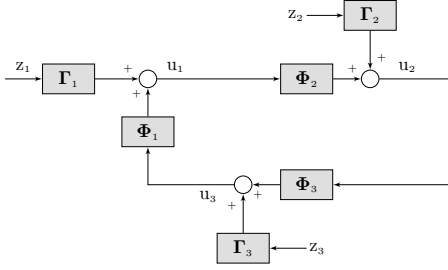


Fig. 2. Three-hop network architecture

Corollary II.7 (Corollary 5.2.3 in [21]). *The set of all closed-loop maps (6) achievable via stabilizing controllers (5) are affine in the Youla parameter \mathbf{Q} and are, moreover, given by*

	r	w	ζ
y	$\mathbf{N}\mathbf{X}_Q$	$\mathbf{N}\mathbf{Y}_Q$	$I_p - \mathbf{N}\mathbf{X}_Q$
u	$\mathbf{M}\mathbf{X}_Q$	$\mathbf{M}\mathbf{Y}_Q - I_m$	$-\mathbf{M}\mathbf{X}_Q$
z	$I_p - \mathbf{N}\mathbf{X}_Q$	$-\mathbf{N}\mathbf{Y}_Q$	$\mathbf{N}\mathbf{X}_Q - I_p$
v	$\mathbf{M}\mathbf{X}_Q$	$\mathbf{M}\mathbf{Y}_Q$	$-\mathbf{M}\mathbf{X}_Q$

(7)

E. Network Realization Functions

For descriptive simplicity, we focus on the three-hop “ring” network from Fig. 2 and we describe its signal flow equations

$$\begin{bmatrix} u_1 \\ u_2 \\ u_3 \end{bmatrix} = \begin{bmatrix} O & O & \Phi_1 \\ \Phi_2 & O & O \\ O & \Phi_3 & O \end{bmatrix} \begin{bmatrix} u_1 \\ u_2 \\ u_3 \end{bmatrix} + \begin{bmatrix} \Gamma_1 & O & O \\ O & \Gamma_2 & O \\ O & O & \Gamma_3 \end{bmatrix} \begin{bmatrix} z_1 \\ z_2 \\ z_3 \end{bmatrix}.$$

Notice that the three by three Φ factor takes the precise meaning of the network’s directed graph *adjacency matrix*, with the LTI filters Φ_1, Φ_2 and Φ_3 , respectively, having the significance of weights of their corresponding edges. The remaining three by three Γ factor has the role of defining the *input terminals* of the network, *i.e.*, the points of access (to the network) of the exogenous signals z_1, z_2 and z_3 , respectively.

Assuming that $(I_m - \Phi)$ is invertible, *i.e.*, the LTI network from Fig. 2 is well-posed, the ensuing left factorization

$$\begin{bmatrix} u_1 \\ u_2 \\ u_3 \end{bmatrix} = \begin{bmatrix} I & O & -\Phi_1 \\ -\Phi_2 & I & O \\ O & -\Phi_3 & I \end{bmatrix}^{-1} \begin{bmatrix} \Gamma_1 & O & O \\ O & \Gamma_2 & O \\ O & O & \Gamma_3 \end{bmatrix} \begin{bmatrix} z_1 \\ z_2 \\ z_3 \end{bmatrix} \quad (8)$$

yields the Input/Output map (from z to u), which we denote by \mathbf{K} . Note that, in general, the sparsity patterns of the Φ and Γ factors are completely lost in (8) due to the inversion of $(I_m - \Phi)$ that generically yields a “full” TFM \mathbf{K} , with no particular sparsity pattern of its own. The distinctive “structure” of the LTI network in Fig. 2, as captured by the (Φ, Γ) pair, cannot in general be retrieved solely from \mathbf{K} (see also [22]).

Remark II.8. *This type of architecture has been successfully employed for the control laws proposed in [15], with the aim of eliminating downstream disturbance propagation for a platoon of autonomous vehicles. Notably, guarantees of closed-loop norm optimality were also obtained in Section V-B of [15].*

Definition II.9. *Given $\mathbf{K} \in \mathbb{R}_p(\lambda)^{m \times p}$, $\Phi \in \mathbb{R}_p(\lambda)^{m \times m}$ and $\Gamma \in \mathbb{R}_p(\lambda)^{m \times p}$ such that Φ has all its diagonal entries equal to zero and $\mathbf{K} = (I_m - \Phi)^{-1}\Gamma$, the pair of TFMs (Φ, Γ) is said to be a Network Realization Function pair of \mathbf{K} .*

Remark II.10. *Notice the fact that any NRF is ultimately a left factorization of \mathbf{K} . For any $\mathbf{K} \in \mathbb{R}_p(\lambda)^{m \times p}$, let $\mathbf{K} = \mathbf{R}^{-1}\mathbf{P}$ be some left factorization (recall Definition II.1). In this case, the gain at infinity of the “denominator” TFM, \mathbf{R} , and that of its diagonal component, \mathbf{R}^{diag} , can always be made (recall Remark II.2) equal to the identity matrix. Therefore, \mathbf{R}^{diag} will have a proper inverse, from which we get that*

$$\left(\Phi := I_m - (\mathbf{R}^{\text{diag}})^{-1}\mathbf{R}, \quad \Gamma := (\mathbf{R}^{\text{diag}})^{-1}\mathbf{P} \right) \quad (9)$$

satisfies Definition II.9, making it an NRF pair of \mathbf{K} . Notably, the transformation from (9) preserves the sparsity patterns: Φ retains the sparsity pattern of \mathbf{R} while Γ retains that of \mathbf{P} .

III. DISTRIBUTED CONTROL VIA NRF IMPLEMENTATION

A. Specifying Sensing and Communication Constraints

The stated aim of this paper is to investigate distributed implementations of output feedback controllers as networks of LTI filters. In the NRF framework, the control law

$$u = \underbrace{\Phi u}_{\text{feedforward}} + \underbrace{\Gamma z}_{\text{feedback}}, \quad (10)$$

which bears striking resemblance to the architecture proposed in (16) from [23], has a twofold manifestation: firstly, in the *sparsity pattern of the Φ factor*, by designating which control signals are available, and secondly, in *that of the Γ factor*, by defining which of the regulated measurements are available.

The communication constraints $\Phi \in \mathcal{Y}$ are imposed on the distributed controller by way of pre-specifying the linear subspace $\mathcal{Y} \subseteq \mathbb{R}_p(\lambda)^{m \times m}$, while the sensing constraints $\Gamma \in \mathcal{X}$ are encapsulated in the pre-specified linear subspace $\mathcal{X} \subseteq \mathbb{R}_p(\lambda)^{m \times p}$, respectively. The subspace \mathcal{Y}^+ is obtained by allowing for non-zero diagonal entries on the elements from \mathcal{Y} such that $\mathbf{Y} \in \mathcal{Y}^+ \iff (\mathbf{Y} - \mathbf{Y}^{\text{diag}}) \in \mathcal{Y}$.

Remark III.1. *In the NRF framework, we avoid communicating internal states, *i.e.*, states of the plant or controller, thus promoting control law implementations that are scalable with respect to the dimension of the plant’s state (recall Section I).*

B. Internal Stability Guarantees

In the NRF-based implementation (10) of the controller, the variable u may be affected by the additive disturbance denoted δ_u , with the equation for the controller from Fig. 3 reading as

$$u = \Phi(u + \delta_u) + \Gamma z. \quad (11)$$

The internal stability analysis must certify that the closed-loop maps from δ_u to the signals z, u, v and y are all stable.

Assumption III.2. *The plant \mathbf{G} is strictly proper.*

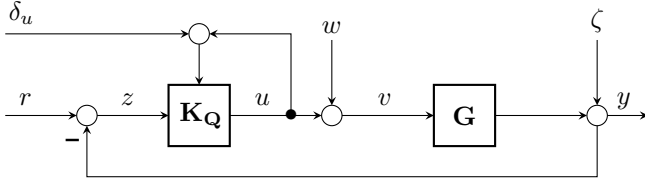


Fig. 3. Feedback loop of the plant \mathbf{G} with the controller \mathbf{K} in an NRF-based implementation $u = \Phi(u + \delta_u) + \Gamma z$

Remark III.3. We point out that Assumption III.2 is by no means restrictive, as shown via [13], and has been made only to facilitate the presentation of the NRF design formalism. For example, a direct consequence of Assumption III.2 is the fact that the TFM s \mathbf{M} , \mathbf{Y} , $\tilde{\mathbf{M}}$, $\tilde{\mathbf{Y}}$ from any DCF of \mathbf{G} can be scaled in (2) to make their gain at infinity equal to the identity matrix. Thus, all DCFs of type (3)-(4) which will be employed in the sequel are taken to have the aforementioned property, implying that $(\mathbf{Y}_{\mathbf{Q}}^{\text{diag}})^{-1} \in \mathbb{R}_p(\lambda)^{m \times m}$ for any $\mathbf{Q} \in \mathbb{R}_{\mathcal{S}}(\lambda)^{m \times p}$.

The next theorem shows that Remark II.10 offers a natural mechanism to obtain stabilizing NRF-based implementations.

Theorem III.4. Let $\mathbf{G} \in \mathbb{R}_p(\lambda)^{p \times m}$ be given by one of its DCFs, as in (2), and define the \mathbf{Q} -parameterized NRF pairs

$$\Phi := I_m - (\mathbf{Y}_{\mathbf{Q}}^{\text{diag}})^{-1} \mathbf{Y}_{\mathbf{Q}}, \quad (12a)$$

$$\Gamma := (\mathbf{Y}_{\mathbf{Q}}^{\text{diag}})^{-1} \mathbf{X}_{\mathbf{Q}}, \quad (12b)$$

associated with a $\mathbf{K}_{\mathbf{Q}}$, as in (5). Then, we have that:

- (a) The NRF-based implementation of $\mathbf{K}_{\mathbf{Q}}$ from (11) internally stabilizes the feedback loop shown in Fig. 3;
- (b) $\Phi \in \mathcal{Y}$, $\Gamma \in \mathcal{X}$ if and only if $\mathbf{Y}_{\mathbf{Q}} \in \mathcal{Y}^+$, $\mathbf{X}_{\mathbf{Q}} \in \mathcal{X}$.

Proof. For point (a), see the Appendix. Point (b) follows directly from the arguments made in Remark II.10. \square

C. Realization-based Distributed Implementations

Distinguishing to the NRF setup, the main result of this section shows that the closed-loop state dynamics from Fig. 3 can be made stable in a distributed fashion, by implementing stabilizable and detectable realizations for each row of $[\Phi \ \Gamma]$. Before extending the input-output stability guarantees given in Section III-B, we first require the next preparatory lemma.

Lemma III.5. Let \mathbf{G}_1 and \mathbf{G}_2 be two proper TFM s , with \mathbf{G}_2 stable and having full row normal rank along with no transmission zeros in $\mathbb{C} \setminus \mathcal{S}$. Then, $\mathcal{P}_u(\mathbf{G}_1 \mathbf{G}_2) = \mathcal{P}_u(\mathbf{G}_1)$.

Proof. See the Appendix. \square

We now formulate the result that shows how to implement distributed and realization-based versions of (11), which successfully stabilize the closed-loop state dynamics from Fig. 3.

Theorem III.6. Let $\mathbf{G} \in \mathbb{R}_p(\lambda)^{p \times m}$ be given by a stabilizable and detectable realization of type (1a)-(1b) and let $\mathbf{K} \in \mathbb{R}_p(\lambda)^{m \times p}$ be an internally stabilizing controller of \mathbf{G} , which is described by an NRF pair (Φ, Γ) as in (12a)-(12b). Then, by implementing stabilizable and detectable realizations for each $e_i^T [\Phi \ \Gamma]$, with $i \in 1 : m$, and by computing the commands as in (11), the closed-loop state dynamics of the system from Fig. 3 will be asymptotically stable (see Section 5.3 in [24]).

Proof. See the Appendix. \square

Remark III.7. By obtaining minimal state-space realizations denoted $e_i^T [\Phi \ \Gamma] = \begin{bmatrix} A_i - \lambda I_{n_i} & B_i \\ C_i & D_i \end{bmatrix}$, $\forall i \in 1 : m$, notice that each zero column of $e_i^T [\Phi \ \Gamma]$ will result in a zero column on the same position in both B_i and D_i , producing structured and stabilizing state-space-based implementations.

Remark III.8. Quite notably, Remark III.7 and Theorem III.6 still hold when implementing minimal and, respectively, stabilizable and detectable realizations for block-rows of $[\Phi \ \Gamma]$, instead of just single rows. Moreover, minimal realizations of such block-rows may also reduce the number of sub-controller states at any location where more than a single command signal is computed, emphasizing the scalability of our method.

We conclude this subsection with the next consequence of Theorem III.6, which certifies closed-loop stability with respect to bounded additive disturbance in dynamics of type (1a)-(1b).

Corollary III.9. Let the same hypotheses and notation hold as in the statement of Theorem III.6. Let the state dynamics (1a) of \mathbf{G} and $[\Phi \ \Gamma]$ be affected additively by the bounded disturbances $\delta_{x_{\mathbf{G}}}$ and $\delta_{x_{\mathbf{K}}}$, respectively, and the output dynamics (1b) of \mathbf{G} and $[\Phi \ \Gamma]$ be affected additively by the bounded disturbances $\delta_{y_{\mathbf{G}}}$ and $\delta_{y_{\mathbf{K}}}$, respectively. Then, all the closed-loop signals and state variables in Fig. 3 remain bounded.

Proof. See the Appendix. \square

Remark III.10. Similarly to the SLS framework from [7], [8], we consider the bounded disturbances $\delta_{x_{\mathbf{K}}}$ and $\delta_{y_{\mathbf{K}}}$ as arising from computational errors and the imperfect implementation of the controller's NRF pair. Moreover, the bounded disturbances $\delta_{x_{\mathbf{G}}}$ and $\delta_{y_{\mathbf{G}}}$ can be attributed to unmapped network dynamics and sources of disturbance which are not captured in (1a)-(1b).

D. Norm-based Optimal Design

Given the sensing and communication subspace constraints \mathcal{X} and \mathcal{Y} , we desire to obtain NRF-based implementations of distributed controllers \mathbf{K} which solve the following problem

$$\min_{\mathbf{K} \in \mathbb{R}(\lambda)^{m \times p}} \|\mathbf{H}_{CL}(\mathbf{G}, \mathbf{K})\| \quad (13a)$$

$$\text{subject to} \quad \text{Fig. 3 is internally stable,} \quad (13b)$$

$$\mathbf{K} = (I_m - \Phi)^{-1} \Gamma, \quad (13c)$$

$$\Phi \in \mathcal{Y}, \Gamma \in \mathcal{X}. \quad (13d)$$

With the difficulty of (13a)–(13d) being well-understood in literature, and its epitome being the computation of an optimal controller having a (block-)diagonal TFM, we now focus on a tractable adaptation of it. The latter is given via the following result, which has the benefit of being stated in terms of affine expressions, starting from a fixed DCF (2) of the plant.

Corollary III.11. Let $\mathbf{G} \in \mathbb{R}_p(\lambda)^{p \times m}$. Consider (Φ, Γ) from (12a)-(12b), based upon a DCF (2) of \mathbf{G} . Then, (13a)–(13d) is equivalent to the following affine model matching problem

$$\min_{\mathbf{Q} \in \mathbb{R}_{\mathcal{S}}(\lambda)^{m \times p}} \|\mathbf{H}_{CL}(\mathbf{G}, \mathbf{K}_{\mathbf{Q}})\| \quad (14a)$$

$$\text{subject to} \quad \mathbf{Y}_{\mathbf{Q}} \in \mathcal{Y}^+, \mathbf{X}_{\mathbf{Q}} \in \mathcal{X}. \quad (14b)$$

Proof. The result follows directly from Theorem III.4. \square

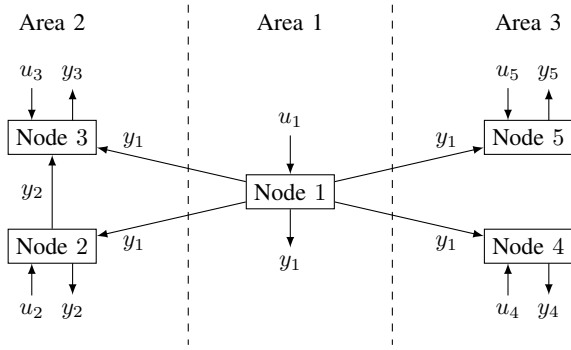


Fig. 4. Interconnection of the network's various nodes and the areas of admissible communication

Remark III.12. Efficient numerical solutions for type (14a)-(14b) problems were proposed in [13]. However, an important limitation of Corollary III.11 is that its outcome depends on the initial choice of a DCF over $\mathbb{R}_S(\lambda)$ for the plant. This was to be expected and has been alleviated in part by the subsequent results from [13]. Similarly, the outcome of the SLS [8] depends on the initial choice of a realization of the plant. Moreover, we point out that the suboptimality gap induced by the desired sparsity structure of Φ and Γ must also be taken into account in the design phase, as is the case with the SLS (see, for example, [4] and the numerical examples from [7]).

IV. ALTERNATIVE REPRESENTATIONS

In this section, we examine the opportunity of implementing NRF-based control schemes as in the SLS framework [7], [8], by employing the closed-loop maps achievable with stabilizing controllers. We denote by $\mathbf{T}_Q^{\ell\epsilon}$ the dependency on the Youla parameter \mathbf{Q} of the closed-loop map between two signals ϵ to ℓ , and let β denote the states of the controller. We investigate a distributed implementation for controllers based on the closed-loop maps from $[\zeta^\top \ r^\top]^\top$ to $[y^\top \ u^\top]^\top$ in Fig. 1, namely

$$\begin{aligned} \mathbf{T}_Q^{y\zeta} \beta &= -\mathbf{T}_Q^{yr} z, \\ u &= \mathbf{T}_Q^{u\zeta} \beta + \mathbf{T}_Q^{ur} z, \end{aligned}$$

or, in terms of the corresponding DCF over $\mathbb{R}_S(\lambda)$, we get that

$$\tilde{\mathbf{Y}}_Q \tilde{\mathbf{M}} \beta = (\tilde{\mathbf{Y}}_Q \tilde{\mathbf{M}} - I_p) z, \quad (15a)$$

$$u = -\tilde{\mathbf{X}}_Q \tilde{\mathbf{M}} \beta + \tilde{\mathbf{X}}_Q \tilde{\mathbf{M}} z. \quad (15b)$$

It can be checked that the elimination of β from (15a)-(15b) (since $\tilde{\mathbf{Y}}_Q \tilde{\mathbf{M}}$ is invertible, as per Remark III.3) yields the \mathbf{K}_Q controller via its right coprime factorization over $\mathbb{R}_S(\lambda)$ $u = \tilde{\mathbf{X}}_Q \tilde{\mathbf{Y}}_Q^{-1} z$, as in (5). For implementation purposes, we require an NRF-based formulation of the ‘‘state iteration’’ from (15a). By applying a transformation of type (9), we get

$$\beta = (I_p - \Omega^{-1} \tilde{\mathbf{Y}}_Q \tilde{\mathbf{M}})(\beta + \delta_\beta) + \Omega^{-1} (\tilde{\mathbf{Y}}_Q \tilde{\mathbf{M}} - I_p) z,$$

where $\Omega := (\tilde{\mathbf{Y}}_Q \tilde{\mathbf{M}})^{\text{diag}}$, which has a proper inverse (recall Remark III.3), while δ_β represents additive disturbances acting upon the controller's states, replacing δ_u from Fig. 3. Thus, we obtain a set of control laws which are akin to the *secondary* specialized implementations from Section III-C of [8], namely

$$\beta = (I_p - \Omega^{-1} \tilde{\mathbf{Y}}_Q \tilde{\mathbf{M}})(\beta + \delta_\beta) + \Omega^{-1} (\tilde{\mathbf{Y}}_Q \tilde{\mathbf{M}} - I_p) z, \quad (16a)$$

$$u = -\tilde{\mathbf{X}}_Q \tilde{\mathbf{M}} \beta + \tilde{\mathbf{X}}_Q \tilde{\mathbf{M}} z. \quad (16b)$$

Yet, as expected (see Section III-C of [8]), this type of specialized implementation for a centralized stabilizing controller is hampered by restrictive assumptions on the plant's TFM.

Theorem IV.1. Let $\mathbf{G} \in \mathbb{R}_p(\lambda)^{p \times m}$ and consider any of its \mathbf{Q} -parameterized DCFs, as in (3)-(4). Define $\Omega := (\tilde{\mathbf{Y}}_Q \tilde{\mathbf{M}})^{\text{diag}}$, where \mathbf{Q} is the (stable) Youla parameter, and let also $\mathbf{K}_Q \in \mathbb{R}_p(\lambda)^{m \times p}$ be a (centralized) stabilizing controller, as in (5). If \mathbf{G} is unstable, then the implementation (16a)-(16b) of \mathbf{K}_Q does not internally stabilize the feedback loop with \mathbf{G} .

Proof. See the Appendix. \square

V. NUMERICAL EXAMPLE

Consider a grid of 5 interconnected nodes separated into 3 local areas, as shown in Fig. 4. We aim to obtain a distributed control law in which each node's controller employs only local measurements and exchanges command values only with other sub-controllers that belong to nodes located in the original node's area or in directly adjacent ones.

Thus, we will devise a control law in which the controller of node 1 sends its command to nodes 2–5 while the controller of node 2 sends its command to node 3. The network from Fig. 4 is modeled as a discrete-time system with a sampling time of $T_s = 100$ ms. To describe the network's TFM, denoted $\mathbf{G}(z)$, define $\Gamma_{\mathbf{G}}(z) := \frac{1}{z-1}$ and $\Phi_{\mathbf{G}}(z) := \frac{0.2}{z-0.8}$ to get that

$$\begin{aligned} \mathbf{B} &:= \begin{bmatrix} 0 & 0 & 0 & 0 & 0 \\ 1 & 0 & 0 & 0 & 0 \\ 1 & 1 & 0 & 0 & 0 \\ 1 & 0 & 0 & 0 & 0 \\ 1 & 0 & 0 & 0 & 0 \end{bmatrix}, & \mathbf{U}(z) &:= I_5 - \Phi_{\mathbf{G}} \mathbf{B}, \\ \mathbf{V}(z) &:= \Gamma_{\mathbf{G}} I_5, & \mathbf{G}(z) &= \mathbf{U}^{-1} \mathbf{V}, \\ \mathbf{U}(z)^{-1} &= \begin{bmatrix} 1 & 0 & 0 & 0 & 0 \\ \Phi_{\mathbf{G}} & 1 & 0 & 0 & 0 \\ \Phi_{\mathbf{G}}^2 + \Phi_{\mathbf{G}} & \Phi_{\mathbf{G}} & 1 & 0 & 0 \\ \Phi_{\mathbf{G}} & 0 & 0 & 1 & 0 \\ \Phi_{\mathbf{G}} & 0 & 0 & 0 & 1 \end{bmatrix}. \end{aligned}$$

Note, moreover, that a DCF over $\mathbb{R}_S(\lambda)$ of \mathbf{G} is given by

$$\begin{aligned} \begin{bmatrix} \tilde{\mathbf{M}} & \tilde{\mathbf{N}} \\ -\tilde{\mathbf{X}} & \tilde{\mathbf{Y}} \end{bmatrix} &= \begin{bmatrix} \frac{z-1}{z-0.5} I_5 & \frac{1}{z-0.5} \mathbf{U}^{-1} \\ \frac{-0.25}{z-0.5} I_5 & \frac{z}{z-0.5} \mathbf{U}^{-1} \end{bmatrix}, \\ \begin{bmatrix} \tilde{\mathbf{Y}} & -\tilde{\mathbf{N}} \\ \tilde{\mathbf{X}} & \tilde{\mathbf{M}} \end{bmatrix} &= \begin{bmatrix} \frac{z}{z-0.5} I_5 & \frac{-1}{z-0.5} I_5 \\ \frac{0.25}{z-0.5} \mathbf{U} & \frac{z-1}{z-0.5} \mathbf{U} \end{bmatrix}. \end{aligned}$$

We choose $\mathbf{Q}(z) = \frac{0.8}{z-0.2} I_5$ to get, for the network from Fig. 4, the control laws from (17), at the top of the next page.

Consider, now, the following simulation scenario. Let the controller (in NRF form) be implemented in standard unity feedback with our network and let the reference signal be given by $r[n] := \mathbf{1}[n] [1 \ 1 \ 1 \ 1 \ 1]^\top$, where $\mathbf{1}[n]$ denotes the discrete-time Heaviside step function.

Also, let each output measurement be disturbed additively by a measurement noise $\zeta_i[n]$, $i \in 1 : 5$, and let each communicated command be affected additively by a communication disturbance $\delta_{ui}[n]$, $i \in 1 : 5$, with these signals being modeled as uniformly distributed noise having $|\zeta_i[n]|, |\delta_{ui}[n]| \leq 0.05$, $\forall n \in \mathbb{N}$. Moreover, let $w_1[n] := 0.5 \times \mathbf{1}[n-20]$ be an additive disturbance at the input of the network's first node.

As can be seen in Fig. 5 on the next page, not only are all signals bounded, even in the presence of communication disturbance, but the distributed controller also ensures satisfactory performance for reference tracking and disturbance rejection.

$$\begin{bmatrix} u_1 \\ u_2 \\ u_3 \\ u_4 \\ u_5 \end{bmatrix} = \begin{bmatrix} 0 & 0 & 0 & 0 & 0 \\ -0.2 & 0 & 0 & 0 & 0 \\ \frac{-0.2z+0.12}{z^2-1.6z+0.64} & \frac{-0.2}{z-0.8} & 0 & 0 & 0 \\ \frac{-0.2}{z-0.8} & 0 & 0 & 0 & 0 \\ \frac{-0.2}{z-0.8} & 0 & 0 & 0 & 0 \end{bmatrix} \begin{bmatrix} u_1 \\ u_2 \\ u_3 \\ u_4 \\ u_5 \end{bmatrix} + \begin{bmatrix} \frac{1.05z-0.85}{z^2-0.2z-0.8} & 0 & 0 & 0 & 0 \\ 0 & \frac{1.05z-0.85}{z^2-0.2z-0.8} & 0 & 0 & 0 \\ 0 & 0 & \frac{1.05z-0.85}{z^2-0.2z-0.8} & 0 & 0 \\ 0 & 0 & 0 & \frac{1.05z-0.85}{z^2-0.2z-0.8} & 0 \\ 0 & 0 & 0 & 0 & \frac{1.05z-0.85}{z^2-0.2z-0.8} \end{bmatrix} \begin{bmatrix} z_1 \\ z_2 \\ z_3 \\ z_4 \\ z_5 \end{bmatrix} \quad (17)$$

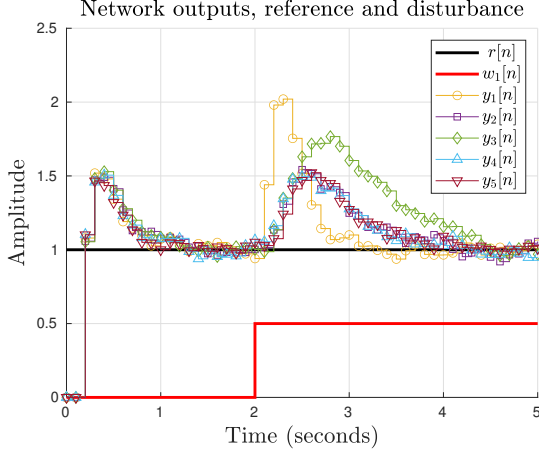


Fig. 5. Reference tracking of the closed-loop network with NRF implementation and input, measurement and communication disturbance

VI. CONCLUSION

We have successfully formalized the distributed design framework introduced in [15], while highlighting its inherent connections [11] with existing techniques from literature [7], [8]. Moreover, we have extended the coprime factor approach from [19] via state-space-based implementations, while laying the theoretic groundwork for reliable numerical procedures [13], enabling the synthesis of scalable and robust control laws.

ACKNOWLEDGMENT

The authors would like to thank our colleague, Dr. Bogdan D. Ciubotaru, for the insightful comments and advice made during the elaboration of this manuscript.

APPENDIX

Proof of Theorem III.4 In order to prove point (a) from the result's statement, we will express all closed-loop maps from $[r^\top \ w^\top \ \zeta^\top \ \delta_u^\top]^\top$ to $[y^\top \ u^\top \ z^\top \ v^\top]^\top$ in terms of the \mathbf{Q} -parameterized DCF given in (3)-(4). The equations of the standard unity feedback interconnection from Fig. 1 are given by $z = r - y$, $v = u + w$, $y = \mathbf{G}v + \zeta$ and $u = \mathbf{K}_\mathbf{Q} z$, respectively, or equivalently by $y = r - z$, $v = u + w$, and

$$z + \mathbf{G}u = -\mathbf{G}w + r - \zeta, \quad (18a)$$

$$-\mathbf{K}_\mathbf{Q}z + u = 0. \quad (18b)$$

Multiplying to the left in (18a) with $\tilde{\mathbf{M}}$ and in (18b) with $\mathbf{Y}_\mathbf{Q}$, we obtain, via the identities from (3)-(4), that

$$\tilde{\mathbf{M}}z + \tilde{\mathbf{N}}u = -\tilde{\mathbf{N}}w + \tilde{\mathbf{M}}r - \tilde{\mathbf{M}}\zeta, \quad (19a)$$

$$-\mathbf{X}_\mathbf{Q}z + \mathbf{Y}_\mathbf{Q}u = 0. \quad (19b)$$

By implementing u via (11) and (12a)-(12b) and allowing it to be affected by δ_u , the equations from (19a)-(19b) turn into

$$\begin{bmatrix} \tilde{\mathbf{M}} & \tilde{\mathbf{N}} \\ -(\mathbf{Y}_\mathbf{Q}^{\text{diag}})^{-1}\mathbf{X}_\mathbf{Q} & (\mathbf{Y}_\mathbf{Q}^{\text{diag}})^{-1}\mathbf{Y}_\mathbf{Q} \end{bmatrix} \begin{bmatrix} z \\ u \end{bmatrix} = \begin{bmatrix} \tilde{\mathbf{M}}r - \tilde{\mathbf{M}}\zeta \\ 0 \end{bmatrix} + \begin{bmatrix} 0 & 0 \\ -\tilde{\mathbf{N}} & \tilde{\mathbf{M}} \\ 0 & 0 \end{bmatrix} \begin{bmatrix} w \\ \zeta \\ \delta_u \end{bmatrix}. \quad (20)$$

To obtain the explicit dependency of $[z^\top \ u^\top]^\top$ in terms of $[r^\top \ w^\top \ \zeta^\top \ \delta_u^\top]^\top$, we multiply (20) to the left with

$$\begin{bmatrix} \tilde{\mathbf{M}} & \tilde{\mathbf{N}} \\ -(\mathbf{Y}_\mathbf{Q}^{\text{diag}})^{-1}\mathbf{X}_\mathbf{Q} & (\mathbf{Y}_\mathbf{Q}^{\text{diag}})^{-1}\mathbf{Y}_\mathbf{Q} \end{bmatrix}^{-1} = \begin{bmatrix} \tilde{\mathbf{Y}}_\mathbf{Q} & -\mathbf{N}\mathbf{Y}_\mathbf{Q}^{\text{diag}} \\ \tilde{\mathbf{X}}_\mathbf{Q} & \mathbf{M}\mathbf{Y}_\mathbf{Q}^{\text{diag}} \end{bmatrix}.$$

Moreover, we have from Fig. 3 that $v = u + w$ and that $y = r - z$. Then, the resulting closed-loop maps will be given by (21), at the top of the next page. Since \mathbf{Q} is stable, all of them will also be stable, thus guaranteeing internal stability. \square

Proof of Lemma III.5 We focus on the case where \mathbf{G}_2 is not a constant matrix and $\mathcal{P}_u(\mathbf{G}_1) \neq \{\emptyset\}$ since, otherwise, the result follows directly from the full row rank of \mathbf{G}_2 , via classical Popov-Belevitch-Hautus (PBH) tests (see Section 3.2 of [24]), or from the stability of \mathbf{G}_1 . We start by expressing \mathbf{G}_1 and \mathbf{G}_2 via the minimal realizations

$$\mathbf{G}_i(\lambda) = \left[\begin{array}{c|c} A_i - \lambda I_{n_i} & B_i \\ \hline C_i & D_i \end{array} \right], \quad i \in \{1, 2\}, \quad (22)$$

and we use these in order to write down the realization of

$$\mathbf{G}_1(\lambda)\mathbf{G}_2(\lambda) = \left[\begin{array}{cc|c} A_1 - \lambda I_{n_1} & B_1 C_2 & B_1 D_2 \\ O & A_2 - \lambda I_{n_2} & B_2 \\ \hline C_1 & D_1 C_2 & D_1 D_2 \end{array} \right], \quad (23)$$

which we will show to be both stabilizable and detectable.

Since \mathbf{G}_2 has full row normal rank and no zeros in $\mathbb{C} \setminus \mathcal{S}$, then by Lemma 3.33 and Theorem 3.34 in [24] and from the minimality of (22), we get that $\mathbf{S}(\lambda) := \begin{bmatrix} A_2 - \lambda I_{n_2} & B_2 \\ C_2 & D_2 \end{bmatrix}$ has full row rank $\forall \lambda \in \mathbb{C} \setminus \mathcal{S}$. From this and the stabilizability of the pair (A_1, B_1) , recalling the minimality of (22), a standard PBH test confirms that (23) is also stabilizable.

From the minimality of (22), we have that the pair (C_1, A_1) is detectable and that $\mathcal{P}_u(\mathbf{G}_2) = \{\emptyset\} \Rightarrow \Lambda_u(A_2) = \{\emptyset\}$. By employing a PBH test, we get that (23) is also detectable, in addition to being stabilizable, and therefore $\mathcal{P}_u(\mathbf{G}_1\mathbf{G}_2) = \Lambda_u(A_1) \cup \Lambda_u(A_2)$. Yet, from the minimality of (22) and by recalling the stability of \mathbf{G}_2 , we have that $\mathcal{P}_u(\mathbf{G}_1) = \Lambda_u(A_1)$ and that $\Lambda_u(A_2) = \{\emptyset\}$. Thus, $\mathcal{P}_u(\mathbf{G}_1\mathbf{G}_2) = \mathcal{P}_u(\mathbf{G}_1)$. \square

Proof of Theorem III.6 The proof can be broken down into four parts. In the first part, (I), we prove that $\mathcal{P}_u([\Phi \ \Gamma]) = \bigcup_{i=1}^m \mathcal{P}_u(e_i^\top [\Phi \ \Gamma])$. By employing this fact along with the stabilizable and detectable realizations denoted

$$e_i^\top [\Phi \ \Gamma] = \left[\begin{array}{c|c} A_i - \lambda I_{n_i} & B_i \\ \hline C_i & D_i \end{array} \right], \quad \forall i \in 1 : m, \quad (24)$$

we prove in part (II) the fact that the resulting realization of the controller's row-based NRF implementation, namely

$$\begin{bmatrix} e_1^\top [\Phi \ \Gamma] \\ \vdots \\ e_i^\top [\Phi \ \Gamma] \\ \vdots \\ e_m^\top [\Phi \ \Gamma] \end{bmatrix} = \left[\begin{array}{cc|c} A_1 - \lambda I_{n_1} & & B_1 \\ & \ddots & \vdots \\ & & A_m - \lambda I_{n_m} & B_m \\ \hline C_1 & & & D_1 \\ & & & \vdots \\ & & & C_m & D_m \end{array} \right], \quad (25)$$

$$\begin{bmatrix} z \\ u \\ v \\ y \end{bmatrix} = \begin{bmatrix} -\tilde{Y}_Q \tilde{N} & \tilde{Y}_Q \tilde{M} & -\tilde{Y}_Q \tilde{M} & N(Y_Q - Y_Q^{\text{diag}}) \\ -\tilde{X}_Q \tilde{N} & \tilde{X}_Q \tilde{M} & -\tilde{X}_Q \tilde{M} & -M(Y_Q - Y_Q^{\text{diag}}) \\ I_m - \tilde{X}_Q \tilde{N} & \tilde{X}_Q \tilde{M} & -\tilde{X}_Q \tilde{M} & -M(Y_Q - Y_Q^{\text{diag}}) \\ \tilde{Y}_Q \tilde{N} & I_p - \tilde{Y}_Q \tilde{M} & \tilde{Y}_Q \tilde{M} & -N(Y_Q - Y_Q^{\text{diag}}) \end{bmatrix} \begin{bmatrix} w \\ r \\ \zeta \\ \delta_u \end{bmatrix} \quad (21)$$

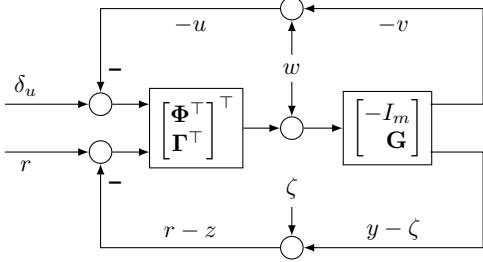


Fig. 6. Equivalent negative unity feedback interconnection

is both stabilizable and detectable. In part (III), we show that the NRF implementation solves a more general stabilization problem and, in part (IV), we employ parts (II) and (III) to prove that these state-space implementations ensure that the closed-loop system's state dynamics are asymptotically stable.

(I) Notice that, since Y_Q^{diag} is a diagonal TFM, we have

$$\begin{aligned} [\Phi \ \Gamma] &= [I_m \ O] - (Y_Q^{\text{diag}})^{-1} [Y_Q \ -X_Q], \\ e_i^T [\Phi \ \Gamma] &= [e_i^T \ O] - e_i^T (Y_Q^{\text{diag}})^{-1} e_i e_i^T [Y_Q \ -X_Q]. \end{aligned}$$

Since $[-X_Q \ Y_Q]$ is stable and since it satisfies (4), then $[-X_Q(\lambda) \ Y_Q(\lambda)]$ has only finite entries along with full row rank $\forall \lambda \in \mathbb{C} \setminus \mathbb{S}$. This means that $[Y_Q \ -X_Q]$ and every $e_i^T [Y_Q \ -X_Q] \forall i \in 1 : m$ will share this property. Then, it follows that $[Y_Q \ -X_Q]$ and every $e_i^T [Y_Q \ -X_Q] \forall i \in 1 : m$ are stable and that they have full row normal rank along with, by Lemma 3.29 in [24], no transmission zeros in $\mathbb{C} \setminus \mathbb{S}$.

We now apply Lemma III.5 to both $(Y_Q^{\text{diag}})^{-1} [Y_Q \ -X_Q]$ and $e_i^T (Y_Q^{\text{diag}})^{-1} e_i e_i^T [Y_Q \ -X_Q]$ in order to get that

$$\begin{aligned} \mathcal{P}_u([\Phi \ \Gamma]) &= \mathcal{P}_u([I_m \ O] - [\Phi \ \Gamma]) = \mathcal{P}_u((Y_Q^{\text{diag}})^{-1}), \\ \mathcal{P}_u(e_i^T [\Phi \ \Gamma]) &= \mathcal{P}_u([e_i^T \ O] - e_i^T [\Phi \ \Gamma]) = \mathcal{P}_u(e_i^T (Y_Q^{\text{diag}})^{-1} e_i). \end{aligned}$$

Moreover, from the diagonal structure of Y_Q^{diag} , it is straightforward to obtain, using classical state-space theory, that $\mathcal{P}_u((Y_Q^{\text{diag}})^{-1}) = \bigcup_{i=1}^m \mathcal{P}_u(e_i^T (Y_Q^{\text{diag}})^{-1} e_i)$. This, in turn, yields the fact that $\mathcal{P}_u([\Phi \ \Gamma]) = \bigcup_{i=1}^m \mathcal{P}_u(e_i^T [\Phi \ \Gamma])$.

(II) We now turn to the stabilizable and detectable realizations for each $e_i^T [\Phi \ \Gamma]$ given in (24). By the stabilizability and detectability of these realizations, we have that $\mathcal{P}_u(e_i^T [\Phi \ \Gamma]) = \Lambda_u(A_i)$. Then, we employ these realizations to form the one from (25) and we define $A_K := \text{diag}(A_1, \dots, A_m)$, which is precisely the state matrix of the realization from (25). By employing the fact that A_K is block-diagonal, we get that $\Lambda_u(A_K) = \bigcup_{i=1}^m \Lambda_u(A_i)$, which implies $\Lambda_u(A_K) = \bigcup_{i=1}^m \mathcal{P}_u(e_i^T [\Phi \ \Gamma]) = \mathcal{P}_u([\Phi \ \Gamma])$. Therefore, it follows (by standard state-space theory) that the realization from (25) must be both detectable and stabilizable.

(III) We now show that $[\Phi \ \Gamma]$ internally stabilizes $[-I_m \ G^T]^T$ in standard unity configuration (recall Fig. 1). Moreover, we point out that this fact is a sufficient condition for the feedback configuration from Fig. 6, which is equivalent to the one in Fig. 3, to be internally stable.

Note that $[\Phi \ \Gamma]$ internally stabilizes $[-I_m \ G^T]^T$ if and only if (see Lemma 5.3 of [24] for the continuous-time positive feedback case) all the entries of the following TFM

$$\tilde{H}_{CL} := \begin{bmatrix} I_m \\ -I_m \\ G \end{bmatrix} \left(I_m + [\Phi \ \Gamma] \begin{bmatrix} -I_m \\ G \end{bmatrix} \right)^{-1} [I_m \ \Phi \ \Gamma] \quad (26)$$

are stable. Recall (3)-(5) along with (12a)-(12b) to get that

$$\tilde{H}_{CL} = [M^T \ -M^T \ N^T]^T [Y_Q^{\text{diag}} \ Y_Q^{\text{diag}} - Y_Q \ X_Q]$$

has only stable entries. Therefore, $[\Phi \ \Gamma]$ internally stabilizes $[-I_m \ G^T]^T$ which also confirms, recalling (21) and the equivalence with Fig. 3, that Fig. 6 is indeed internally stable.

(IV) Finally, recall from the result's statement that the plant is described by a stabilizable and detectable realization

$$\sigma x_G = Ax_G + Bu_G, \quad (27a)$$

$$y_G = Cx_G + Du_G, \quad (27b)$$

and then denote the realization of $[\Phi \ \Gamma]$ from (25) as follows

$$\sigma x_K = A_K x_K + B_1 u_{K1} + B_2 u_{K2}, \quad (28a)$$

$$y_K = C_K x_K + D_1 u_{K1} + D_2 u_{K2}. \quad (28b)$$

With these representations, it is straightforward to check by direct substitution that the closed-loop state dynamics of type (1a)-(1b) in Fig. 3 are described by the same set of equations (with respect to the same sets of inputs and outputs) as those in Fig. 6 when $[-I_m \ G^T]^T$ is described by the realization

$$\sigma x_G = Ax_G + Bu_G, \quad (29a)$$

$$-u_G = Ox_G - I_m u_G, \quad (29b)$$

$$y_G = Cx_G + Du_G. \quad (29c)$$

Note that, since (27a)-(27b) is stabilizable and detectable, then so is (29a)-(29c) and that these two realizations share the same state variables, *i.e.*, the components of the plant's state vector.

Consider the state vector of the closed-loop interconnections in both Fig. 3 and in Fig. 6 to be the concatenation of the plant's state vector, x_G , with the distributed controller's state vector, x_K . Following this, define $\tilde{D} := \begin{bmatrix} I_m & O & I_m \\ O & I_p & -D \\ D_{K1} & D_{K2} & I_m \end{bmatrix}$. To show that \tilde{D} is invertible, we compute the Schur complement of its upper left $(m+p) \times (m+p)$ block and obtain

$$\begin{aligned} I_m + [D_{K1} \ D_{K2}] [-I_m \ D^T]^T &= \\ &= I_m + [\Phi(\infty) \ \Gamma(\infty)] [-I_m \ G^T(\infty)]^T. \end{aligned} \quad (30)$$

Since $I_m + [\Phi \ \Gamma] [-I_m \ G^T]^T$ is proper and its inverse is, by point (III), both proper and stable, then the Schur complement from (30) is invertible, implying that \tilde{D} is also invertible. We now combine (27a)-(27b) and (29a)-(29c) with (28a)-(28b) to get the fact that the closed-loop interconnection's realization in both Fig. 3 and in Fig. 6 has the following state matrix

$$\begin{bmatrix} \sigma x_{\mathbf{G}} \\ \sigma x_{\mathbf{K}} \end{bmatrix} = A_{CL} \begin{bmatrix} x_{\mathbf{G}} \\ x_{\mathbf{K}} \end{bmatrix} + \begin{bmatrix} O & O & B \\ -B_{\mathbf{K}1} & -B_{\mathbf{K}2} & O \end{bmatrix} \tilde{D}^{-1} \begin{bmatrix} O & I_m & O & -I_m & O & O \\ -I_p & O & I_p & O & I_p & O \\ O & I_m & O & O & O & I_m \end{bmatrix} \begin{bmatrix} r^\top & w^\top & \zeta^\top & \delta_u^\top & \delta_{y_{\mathbf{G}}}^\top & \delta_{y_{\mathbf{K}}}^\top \end{bmatrix}^\top + \begin{bmatrix} \delta_{x_{\mathbf{G}}} \\ \delta_{x_{\mathbf{K}}} \end{bmatrix} \quad (32)$$

$$A_{CL} = \begin{bmatrix} A & O \\ O & A_{\mathbf{K}} \end{bmatrix} + \begin{bmatrix} O & O & B \\ -B_{\mathbf{K}1} & -B_{\mathbf{K}2} & O \end{bmatrix} \tilde{D}^{-1} \begin{bmatrix} O & O \\ C & O \\ O & C_{\mathbf{K}} \end{bmatrix}. \quad (31)$$

Since the TFM from (26) is stable, while (29a)-(29c) and (28a)-(28b) are stabilizable and detectable, we apply the negative unity feedback versions of Lemmas 5.2 and 5.3 from [24] to the feedback loop from Fig. 6 (directly in the continuous-time case and in adapted form for discrete-time) to get that $\Lambda_u(A_{CL}) = \{\emptyset\}$. This is equivalent, by Definition 5.2 in [24] (with the appropriate alteration for the discrete-time case), to the desired result, *i.e.*, the two state vectors, $x_{\mathbf{G}}$ and $x_{\mathbf{K}}$, in Fig. 3 or in Fig. 6 are driven asymptotically to the zero vector, when evolving freely from any finite initial conditions. \square

Proof of Corollary III.9 We start by recalling the realizations from (27a)-(27b) and (28a)-(28b), along with the matrix A_{CL} from (31). As discussed in part (IV) of the proof belonging to Theorem III.6, the closed-loop state dynamics of type (1a) in Fig. 3, when considering the closed-loop state variables to be the concatenation of $x_{\mathbf{G}}$ (the state vector of \mathbf{G}) and of $x_{\mathbf{K}}$ (the state vector of $[\Phi \quad \Gamma]$), are given by (32) at the top of this page. Since $\Lambda_u(A_{CL}) = \{\emptyset\}$, the closed-loop system in Fig. 3 is guaranteed to be internally stable, even when taking into account the bounded disturbances from the statement. \square

Proof of Theorem IV.1 The proof boils down to showing the fact that the closed-loop map from the input disturbance w to the controller's state β , denoted $\mathbf{T}_{\mathbf{Q}}^{\beta w}$, is unstable if so is \mathbf{G} .

Begin with the closed-loop equations, which are given by

$$\tilde{\mathbf{M}}z + \tilde{\mathbf{N}}u = -\tilde{\mathbf{N}}w + \tilde{\mathbf{M}}r - \tilde{\mathbf{M}}\zeta, \quad (33a)$$

$$\Omega^{-1}(I_p - \tilde{\mathbf{Y}}_{\mathbf{Q}}\tilde{\mathbf{M}})z + \Omega^{-1}\tilde{\mathbf{Y}}_{\mathbf{Q}}\tilde{\mathbf{M}}\beta = (I_p - \Omega^{-1}\tilde{\mathbf{Y}}_{\mathbf{Q}}\tilde{\mathbf{M}})\delta_{\beta}, \quad (33b)$$

$$\tilde{\mathbf{X}}_{\mathbf{Q}}\tilde{\mathbf{M}}z - \tilde{\mathbf{X}}_{\mathbf{Q}}\tilde{\mathbf{M}}\beta - u = O, \quad (33c)$$

where (33b)-(33c) represent the distributed implementation of the controller. Next, multiply (33a) to the left with $\tilde{\mathbf{Y}}_{\mathbf{Q}}$ and rewrite (33a)-(33c) in matrix form in order to get that

$$\begin{bmatrix} \tilde{\mathbf{Y}}_{\mathbf{Q}}\tilde{\mathbf{M}} & O & \tilde{\mathbf{Y}}_{\mathbf{Q}}\tilde{\mathbf{N}} \\ \Omega^{-1}(I_p - \tilde{\mathbf{Y}}_{\mathbf{Q}}\tilde{\mathbf{M}}) & \Omega^{-1}\tilde{\mathbf{Y}}_{\mathbf{Q}}\tilde{\mathbf{M}} & O \\ \tilde{\mathbf{X}}_{\mathbf{Q}}\tilde{\mathbf{M}} & -\tilde{\mathbf{X}}_{\mathbf{Q}}\tilde{\mathbf{M}} & -I_m \end{bmatrix} \begin{bmatrix} z \\ \beta \\ u \end{bmatrix} = \begin{bmatrix} -\tilde{\mathbf{Y}}_{\mathbf{Q}}\tilde{\mathbf{N}} & \tilde{\mathbf{Y}}_{\mathbf{Q}}\tilde{\mathbf{M}} & -\tilde{\mathbf{Y}}_{\mathbf{Q}}\tilde{\mathbf{M}} & O \\ O & O & O & I_p - \Omega^{-1}\tilde{\mathbf{Y}}_{\mathbf{Q}}\tilde{\mathbf{M}} \\ O & O & O & O \end{bmatrix} \begin{bmatrix} w \\ r \\ \zeta \\ \delta_{\beta} \end{bmatrix}. \quad (34)$$

The expression of the closed-loop maps can be obtained by multiplying (34) to the left with the inverse of the square TFM on the left-hand side. Doing so, we get the fact that $\mathbf{T}_{\mathbf{Q}}^{\beta w} = \mathbf{G}\tilde{\mathbf{X}}_{\mathbf{Q}}\tilde{\mathbf{N}}$ and by employing the identity $\tilde{\mathbf{X}}_{\mathbf{Q}}\tilde{\mathbf{N}} = I_m - \mathbf{M}\mathbf{Y}_{\mathbf{Q}}$, which can be deduced from (4), we finally obtain the fact that $\mathbf{T}_{\mathbf{Q}}^{\beta w} = \mathbf{G}(I_m - \mathbf{M}\mathbf{Y}_{\mathbf{Q}}) = \mathbf{G} - \mathbf{N}\mathbf{M}^{-1}\mathbf{M}\mathbf{Y}_{\mathbf{Q}} = \mathbf{G} - \mathbf{N}\mathbf{Y}_{\mathbf{Q}}$.

If \mathbf{G} is unstable, then so is $\mathbf{T}_{\mathbf{Q}}^{\beta w}$ for any stable \mathbf{Q} , since $\mathbf{N}\mathbf{Y}_{\mathbf{Q}}$ is guaranteed to be stable, thus making the implementations in (16a)-(16b) unable to stabilize the feedback loop. \square

REFERENCES

- [1] R. A. Date and J. H. Chow, "Decentralized Stable Factors and a Parametrization of Decentralized Controllers," *IEEE Transactions on Automatic Control*, vol. 39, no. 2, pp. 347–351, 1994.
- [2] G. Fazelnia, R. Madani, A. Kalbat, and J. Lavaei, "Convex Relaxation for Optimal Distributed Control Problems," *IEEE Transactions on Automatic Control*, vol. 62, no. 1, pp. 206–221, 2017.
- [3] F. Lin, M. Fardad, and M. R. Jovanovic, "Design of Optimal Sparse Feedback Gains via the Alternating Direction Method of Multipliers," *IEEE Transactions on Automatic Control*, vol. 58, pp. 2426–2431, 2013.
- [4] N. Matni and V. Chandrasekaran, "Regularization for Design," *IEEE Transactions on Automatic Control*, vol. 61, no. 12, pp. 3991–4006, 2016.
- [5] Y. Wang, J. A. Lopez, and M. Sznaier, "Convex Optimization Approaches to Information Structured Decentralized Control," *IEEE Transactions on Automatic Control*, vol. 63, no. 10, pp. 3393–3403, 2018.
- [6] M. Naghnaei, P. Voulgaris, and N. Elia, "A Youla Operator State-Space Framework for Stably Realizable Distributed Control," pp. 1–16, 2019. [Online]. Available: <https://arxiv.org/abs/1910.01045>
- [7] Y.-S. Wang, N. Matni, and J. C. Doyle, "Separable and Localized System-Level Synthesis for Large-Scale Systems," *IEEE Transactions on Automatic Control*, vol. 63, no. 12, pp. 4234–4249, 2018.
- [8] —, "A System-Level Approach to Controller Synthesis," *IEEE Transactions on Automatic Control*, vol. 64, no. 10, pp. 4079–4093, 2019.
- [9] S. Boyd, C. Baratt, and S. Norman, "Linear controller design: limits of performance via convex optimization," *In Proc. of the IEEE*, vol. 78, no. 3, pp. 529–574, 1990.
- [10] L. Furieri, Y. Zheng, A. Papachristodoulou, and M. Kamgarpour, "An Input–Output Parametrization of Stabilizing Controllers: Amidst Youla and System Level Synthesis," *IEEE Control Systems Letters*, vol. 3, no. 4, pp. 1014–1019, 2019.
- [11] Y. Zheng, L. Furieri, A. Papachristodoulou, N. Li, and M. Kamgarpour, "On the Equivalence of Youla, System-Level, and Input–Output Parametrizations," *IEEE Transactions on Automatic Control*, vol. 66, no. 1, pp. 413–420, 2021.
- [12] S.-H. Tseng, "Realization, Internal Stability, and Controller Synthesis," *In Proc. of the 2021 American Control Conference*, 2021.
- [13] A. Sperilă, C. Oară, B. D. Ciubotaru, and Ş. Sabău, "Distributed Control of Descriptor Networks: A Convex Procedure for Augmented Sparsity," *IEEE Transactions on Automatic Control*, to be published, 2024.
- [14] S.-H. Tseng and J. Anderson, "Deployment Architectures for Cyber-Physical Control Systems," *In Proc. of the 2020 American Control Conference*, pp. 5287–5294, 2020.
- [15] Ş. Sabău, C. Oară, S. Warnick, and A. Jadbabaie, "Optimal Distributed Control for Platooning via Sparse Coprime Factorizations," *IEEE Transactions on Automatic Control*, vol. 62, no. 1, pp. 305–320, 2017.
- [16] E. Yeung, J. M. Goncalves, H. Sandberg, and S. Warnick, "The Meaning of Structure in Interconnected Dynamic Systems," pp. 1–21, 2011, [Online]. Available: <http://arxiv.org/abs/1108.2755>.
- [17] Y. Yuan, G.-B. Stan, S. Warnick, and J. Goncalves, "Robust dynamical network structure reconstruction," *Automatica*, vol. 47, no. 6, pp. 1230–1235, 2011.
- [18] Ş. Sabău, A. Sperilă, C. Oară, and A. Jadbabaie, "Sparse Representations of Dynamical Networks: A Coprime Factorization Approach," pp. 1–16, 2022, [Online]. Available: <https://arxiv.org/abs/2206.09945>.
- [19] L. Furieri, Y. Zheng, A. Papachristodoulou, and M. Kamgarpour, "Sparsity Invariance for Convex Design of Distributed Controllers," *IEEE Transactions on Control of Network Systems*, vol. 7, no. 4, pp. 1836–1847, 2020.
- [20] T. Kailath, *Linear Systems*. Prentice-Hall, 1980.
- [21] M. Vidyasagar, *Control System Synthesis: A Factorization Approach, Part I*. MIT Press, Signal Proc., Optimization, and Control Ser., 1985.
- [22] H. H. Weerts, P. M. V. den Hof, and A. G. Dankers, "Identifiability of linear dynamic networks," *Automatica*, vol. 89, pp. 247–258, 2018.
- [23] Y.-S. Wang, N. Matni, S. You, and J. C. Doyle, "Localized distributed state feedback control with communication delays," *In Proc. of the 2014 American Control Conference*, pp. 5748–5755, 2014.
- [24] K. Zhou, J. Doyle, and K. Glover, *Robust and Optimal Control*. Prentice-Hall, 1996.